

**AFRL-ML-WP-TP-2007-545**

**NEW PHENOMENA IN DYE-DOPED  
LIQUID CRYSTALS: BLACK HOLE  
EFFECT AND SWITCHABLE  
REVERSED DIFFRACTION (Postprint)**



**D.R. Evans, G. Cook, M.A. Saleh, J.L. Carns, S. Serak, and N. Tabiryan**

**JANUARY 2006**

**Approved for public release; distribution unlimited.**

**STINFO COPY**

**©2006 Taylor & Francis Group, LLC**

**The U.S. Government is joint author of this work and has the right to use, modify, reproduce, release, perform, display, or disclose the work.**

**MATERIALS AND MANUFACTURING DIRECTORATE  
AIR FORCE RESEARCH LABORATORY  
AIR FORCE MATERIEL COMMAND  
WRIGHT-PATTERSON AIR FORCE BASE, OH 45433-7750**

REPORT DOCUMENTATION PAGE				Form Approved OMB No. 0704-0188	
<p>The public reporting burden for this collection of information is estimated to average 1 hour per response, including the time for reviewing instructions, searching existing data sources, gathering and maintaining the data needed, and completing and reviewing the collection of information. Send comments regarding this burden estimate or any other aspect of this collection of information, including suggestions for reducing this burden, to Department of Defense, Washington Headquarters Services, Directorate for Information Operations and Reports (0704-0188), 1215 Jefferson Davis Highway, Suite 1204, Arlington, VA 22202-4302. Respondents should be aware that notwithstanding any other provision of law, no person shall be subject to any penalty for failing to comply with a collection of information if it does not display a currently valid OMB control number. <b>PLEASE DO NOT RETURN YOUR FORM TO THE ABOVE ADDRESS.</b></p>					
1. REPORT DATE (DD-MM-YY) January 2006		2. REPORT TYPE Journal Article Postprint		3. DATES COVERED (From - To)	
4. TITLE AND SUBTITLE  NEW PHENOMENA IN DYE-DOPED LIQUID CRYSTALS: BLACK HOLE EFFECT AND SWITCHABLE REVERSED DIFFRACTION (Postprint)				5a. CONTRACT NUMBER IN-HOUSE	
				5b. GRANT NUMBER	
				5c. PROGRAM ELEMENT NUMBER 62102F	
6. AUTHOR(S) D.R. Evans, (Agile Filters Project, Exploratory Development) G. Cook (Universal Technology Corp.) M.A. Saleh (UES, Inc.) J.L. Carns (Anteon Corp.) S. Serak and N. Tabiryan (BEAM Engineering for Advanced Measurements Co.)				5d. PROJECT NUMBER 4348	
				5e. TASK NUMBER RG	
				5f. WORK UNIT NUMBER M08R1000	
7. PERFORMING ORGANIZATION NAME(S) AND ADDRESS(ES)  Agile Filters Project, Exploratory Development, Hardened Materials Branch Survivability and Sensor Materials Division, Materials and Manufacturing Directorate Air Force Research Laboratory, Air Force Materiel Command Wright-Patterson Air Force Base, OH 45433-7750				8. PERFORMING ORGANIZATION REPORT NUMBER  AFRL-ML-WP-TP-2007-545  - Universal Technology Corp. - UES Inc. - Anteon Corp. - BEAM Engineering for Advanced Measurements Co.	
9. SPONSORING/MONITORING AGENCY NAME(S) AND ADDRESS(ES) Materials And Manufacturing Directorate Air Force Research Laboratory Air Force Materiel Command Wright-Patterson Air Force Base, OH 45433-7750				10. SPONSORING/MONITORING AGENCY ACRONYM(S) AFRL/MLPJ	
				11. SPONSORING/MONITORING AGENCY REPORT NUMBER(S) AFRL-ML-WP-TP-2007-545	
12. DISTRIBUTION/AVAILABILITY STATEMENT Approved for public release; distribution unlimited.					
13. SUPPLEMENTARY NOTES ©2006 Taylor & Francis Group, LLC. The U.S. Government is joint author of this work and has the right to use, modify, reproduce, release, perform, display, or disclose the work. PAO case number AFRL/WS 06-0320, 07 February 2006. Published in Molecular Crystals & Liquid Crystals 2006, Vol. 453. Paper contains color.					
14. ABSTRACT A nonlinear extinction of transmitted light is observed in liquid crystal cells with large concentrations of anthraquinone dye. Two distinct mechanisms are responsible for this effect when exposed to low and high intensity light, respectively. At low intensities, critical opalescence, micro-scatter, and an increase in linear absorption occur; whereas high intensities result in scattering from photo-induced micro-bubbles.					
15. SUBJECT TERMS anthraquinone dye, bubbles, critical opalescence, light scattering, liquid crystals, Marangoni effect, micro-domains, nonlinear transmission					
16. SECURITY CLASSIFICATION OF:			17. LIMITATION OF ABSTRACT: SAR	18. NUMBER OF PAGES 20	19a. NAME OF RESPONSIBLE PERSON (Monitor) Dean R. Evans 19b. TELEPHONE NUMBER (Include Area Code) (937) 255-4588
a. REPORT Unclassified	b. ABSTRACT Unclassified	c. THIS PAGE Unclassified			

## **New Phenomena in Dye-Doped Liquid Crystals: Black Hole Effect and Switchable Reversed Diffraction**

### **D. R. Evans**

Air Force Research Laboratory, Materials and Manufacturing  
Directorate Wright-Patterson Air Force Base, Ohio

### **G. Cook**

Air Force Research Laboratory, Materials and Manufacturing  
Directorate Wright-Patterson Air Force Base, Ohio and Universal  
Technology Corporation, Dayton, Ohio

### **M. A. Saleh**

Air Force Research Laboratory, Materials and Manufacturing  
Directorate Wright-Patterson Air Force Base, Ohio and UES, Inc.,  
Dayton, Ohio

### **J. L. Carns**

Air Force Research Laboratory, Materials and Manufacturing  
Directorate Wright-Patterson Air Force Base, Ohio and  
Anteon Corporation, Dayton, Ohio

### **S. Serak**

### **N. Tabiryan**

BEAM Engineering for Advanced Measurements Co.,  
Winter Park, Florida

*A nonlinear extinction of transmitted light is observed in liquid crystal cells with large concentrations of anthraquinone dye. Two distinct mechanisms are responsible for this effect when exposed to low and high intensity light, respectively. At low intensities, critical opalescence, micro-scatter, and an increase in linear absorption occur; whereas high intensities result in scattering from photo-induced micro-bubbles.*

The authors would like to thank Kevin Cissner, Roger Becker, and Richard Sutherland for useful discussion and David Zelmon for the use of an integrating sphere.

Address correspondence to Dean R. Evans, Air Force Research Laboratory, Materials and Manufacturing Directorate, Wright-Patterson Air Force Base, Ohio 45433. E-mail: dean.evans@wpafb.af.mil

**Keywords:** anthraquinone dye; bubbles; critical opalescence; light scattering; liquid crystals; Marangoni effect; micro-domains; nonlinear transmission

## INTRODUCTION

One of the more important developments in nonlinear optics of liquid crystals (LCs), following the discovery of the orientational mechanism of optical nonlinearity [1–3], is the comprehension that the nonlinear refraction of LCs could be enhanced by one to two orders of magnitude due to the addition of certain dyes. These enhancements of the optical nonlinearities have been observed with dye concentrations as low as 0.1 wt.% [4–6]. The presence of dyes in LCs has been shown to be an effective means of increasing the nonlinear extinction of radiation due to physical processes such as absorption or scattering [7–9].

Large concentrations of dye in LCs have not been investigated to the same level as weakly doped materials. In the present paper we show that increasing the dye concentration of anthraquinone (AQ) doped LCs to saturation levels results in new intricate processes of light extinction and scattering. The physical mechanisms responsible for these processes have been determined to be rather different for low and high intensities of laser light. At low intensities, the transmitted light appears to vanish under certain conditions due to critical opalescence, formation of micro-domains and enhanced absorption, and has been dubbed the “Black Hole” effect. Above a critical pump intensity, the light is abruptly back-scattered due to the generation of micro-bubbles invoking the term “Switchable Reversed Diffraction” (SRD).

## MATERIAL AND EXPERIMENTAL DESCRIPTION

LC cells consisting of 4-pentyl-4'-cyanobiphenyl (5CB), with thicknesses of 30  $\mu\text{m}$ , 50  $\mu\text{m}$ , and 80  $\mu\text{m}$ , were doped with various concentrations of 1,8-dihydroxy,4,5-diamino,2,7-diisopentyl-anthraquinone (AQ) dye ranging from 0.3 wt.% to 2.0 wt.%. The molecular structures of both the host LC (5CB) and the AQ dye are shown in Figure 1. The glass substrates were covered with 0.5 wt.% solution of poly(vinylalcohol) (PVA) in distilled water and spin-coated for 30 s at 4000 rpm. The PVA films dried at 80°C for 20 minutes and were then rubbed anti-parallel with a cloth to yield a planar alignment. The 30  $\mu\text{m}$  thick LC cells were doped with various concentrations (0.3, 0.6, 0.75, 0.85, 1.0, 1.2, and 1.5 wt.%) of AQ dye, which were used to determine the influence of the linear absorption on the black hole effect. The 50  $\mu\text{m}$  thick cells, doped with either 1.2 wt.% or 2.0 wt.% AQ dye, were used

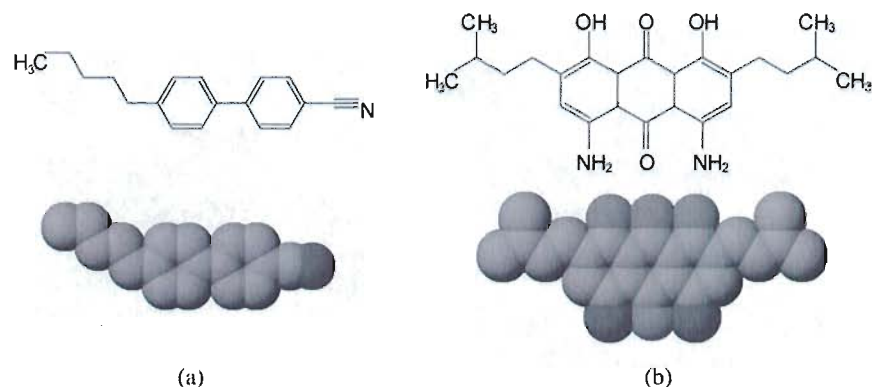


**FIGURE 1** The structural formula and modeling of the molecules of the component materials: (a) nematic liquid crystal 4-pentyl-4'-cyanobiphenyl (5CB); (b) anthraquinone dye: 1,8-dihydroxy,4,5-diamino,2,7-diisopentyl-anthraquinone.

for the investigation of the scattering effects, micro-domains and critical opalescence, associated with the black hole effect. The 80  $\mu\text{m}$  thick cell contained 2.0 wt. % AQ dye and was used for the study of the SRD effect.

Several different experiments were conducted for this study. Absorption spectroscopy was used to compare the effects of concentration on the linear absorption of the nematic and isotropic phases. The dynamics of both the black hole and SRD effects were characterized using either an unpolarized continuous wave (CW) 633 nm He-Ne laser (Coherent 31-2082-000) or a linearly polarized CW 532 nm laser (Coherent Verdi), respectively. Near-field images of these effects were observed with a CCD camera; the experimental arrangement used for collecting these images is shown in Figure 2a. A Hitachi KP20B CCD was used for the investigation of the black hole effect, whereas a Sony DC-77RR CCD was used for the investigation of the SRD. Far-field images were observed in a similar manner where the light transmitted through the LC cell onto a screen; without the use of the white light source, 10X microscope objective, notch filter, and CCD camera as shown in Figure 2a. To quantify the SRD effect in the thick cell, both transmission and reflection measurements were conducted using an integrating sphere, where the cell was placed at normal incidence in the focal plane as shown in Figures 2b,c. Because of the thickness and large absorption coefficient of the cell used for the SRD effect studies, 532 nm was selected in order to reduce the absorbance. The hysteresis curve of the divergence angle as a function of input power, as related to the SRD effect, was measured in the

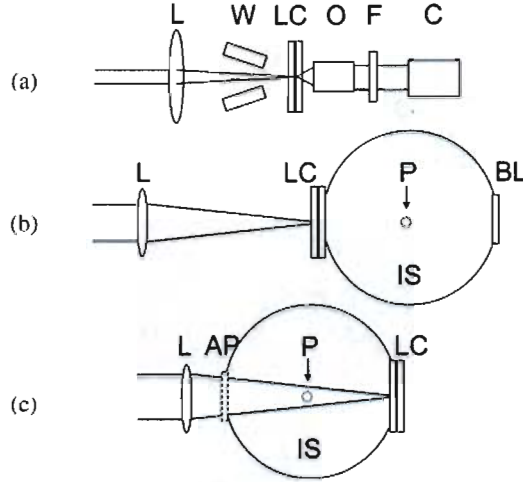


**FIGURE 2** The experimental arrangements for near-field imaging (a) and integrated power measurements (b,c). The arrangement in schematic (a) consists of a lens (L), a liquid crystal cell (LC), a white light source (W), a microscope objective (O), a notch filter (F), and a CCD camera (C). The arrangement in schematics (b,c) consist of a lens (L), a liquid crystal cell (LC), an integrating sphere (IS), and an external power detector (P). Arrangement (b) is used for transmission measurements, where a blank cover (BL) is on the exit port. Arrangement (c) is used for reflection measurements where an aperture (AP) is used on the entrance port and an external power detector placed at the port on the bottom side of the integrating sphere (P).

same cell using a 35 mm focal length lens ( $f/47$ ) to focus the laser light onto the sample. The transmitted beam was viewed on a screen placed 36 mm behind the LC cell. Except where specified, the focusing conditions used were  $f/27$  and  $f/14$  for the black hole and SRD measurements, respectively.

## RESULTS AND DISCUSSION

### Part 1-Black Hole Effect

The black hole effect is described in Figure 3, where the laser beam exiting of the LC cell is shown for various positions of the cell with respect to the focal plane. At weak intensities ( $<1 \text{ W/cm}^2$ ) light is transmitted through the cell without undergoing nonlinear effects (Fig. 3a,e). Increasing the intensity of light on the LC cell results in local heating, which changes the LC/dye mixture from a nematic to an isotropic phase. At higher intensities ( $>10 \text{ kW/cm}^2$ ), when the cell

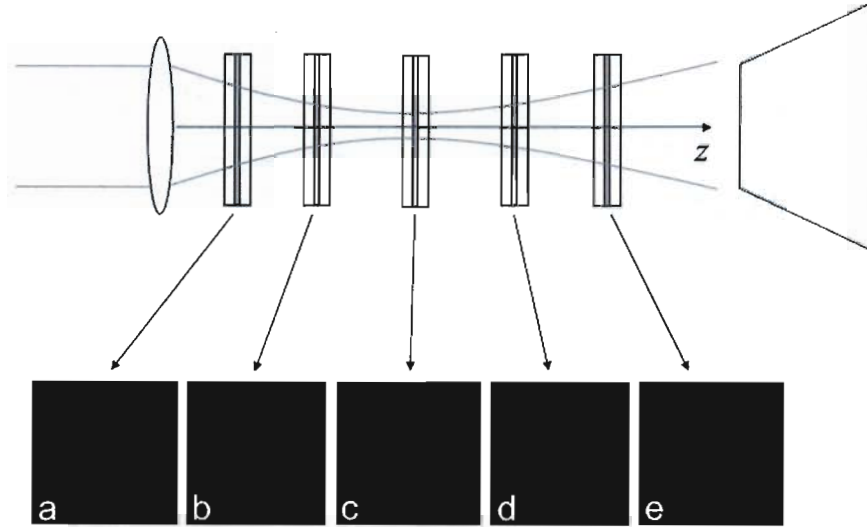


**FIGURE 3** Far-field image of the transmitted light: (a,e) Normal transmission, (b,d) black hole effect, and (c) self phase modulation.

is placed at the beam waist, self phase modulation occurs, as shown in Figure 3c. This is apparent by the typical nonlinear phase modulation pattern observed in the far-field [1–3]. In between these positions at an intermediate focal position (Figs. 3b,d), where the incident intensity is  $\sim 10 \text{ W/cm}^2$ , the transmitted beam disappears. Although it is not shown in Figure 3 at intermediate positions (between positions A and B and positions D and E) a single ring forms, which we believe is due to the threshold of self-focusing giving rise to an on-axis intensity spike in the near field and the Fourier transform of this in the far field (a single ring). Upon recollimation, the beam quality is restored indicating the average phase profile is not significantly distorted. The transmission of the 2.0 wt.% AQ doped LC cell as a function of distance from focus for different incident powers is shown in Figure 4; the cell was translated at  $450 \mu\text{m/s}$ . At low power levels the transmission reaches a minimum at the focal plane of the lens and decreases with increasing incident power. Starting from around  $4 \text{ mW}$ , the transmission in the focus increases with increasing power. The effect of a decreasing transmission at such higher power values is further observed in the vicinity, however, at a distance from the focus.

There are several mechanisms considered to be associated with the black hole effect: micro-domain scatter, critical opalescence, and enhanced absorption. Figure 5 shows the effect of the micro-domain

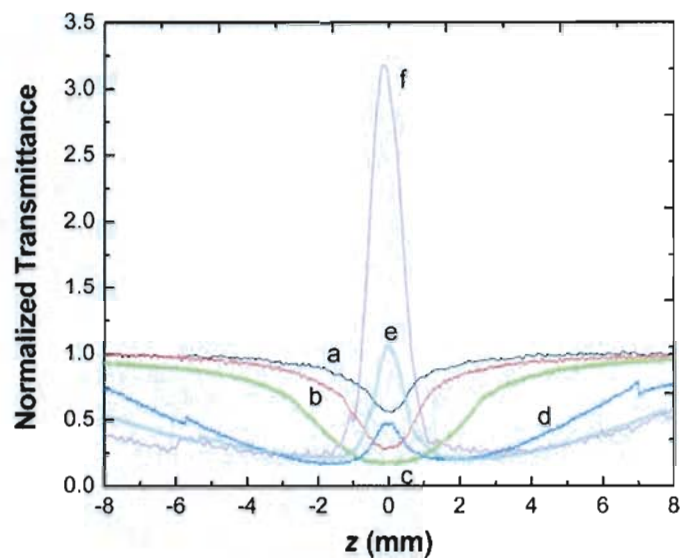


**FIGURE 4** Transmission of the 2 wt.% AQ doped LC cell as a function of distance from focus for different powers of an unpolarized 633 nm laser beam. The powers used were (a) 0.5 mW, (b) 0.7 mW, (c) 1.7 mW, (d) 3.8 mW, (e) 5.2 mW, and (f) 9.3 mW.

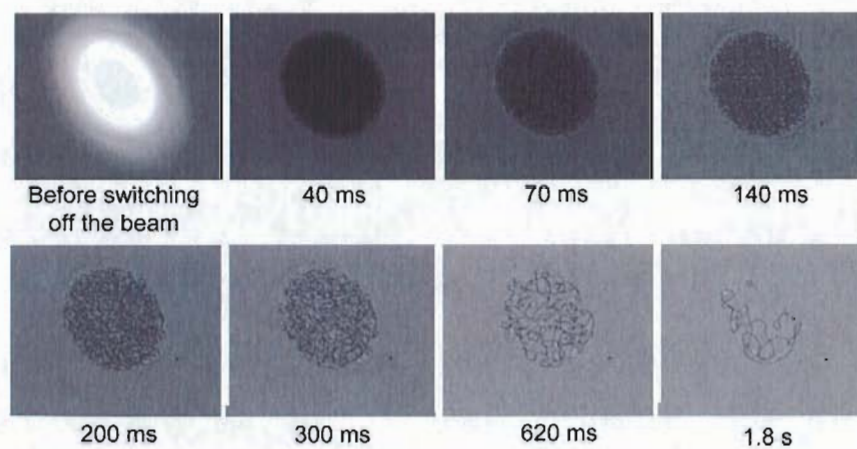


**FIGURE 5** Near-field images of the micro-domain structure as a function of time. The times listed correspond to the duration of time past since the laser beam was removed.



scatter, where heat generated from the strong absorption of the dye drives the LC molecules to the phase transition point. A laser beam of 14.4 mW power was focused onto a 50 mm cell using an f/80 focusing optics was used in these tests. In order to observe the domain structure, the LC cell was placed between crossed-polarizers on a microscope stage such that the LC director was at  $45^\circ$  with respect to the polarizers. The near-field images were viewed using a 10X microscope objective and a CCD camera. Immediately after the laser beam was removed, a large density of micro-domains was observed. These micro-domains are attributed to both random local orientations in the nematic phase and a mixture of nematic and isotropic phases. On the order of 100 ms after the laser beam was switched off, there was a reduction in the density of these micro-domains; several seconds later the micro-domains vanished. Although the role of the dye in this process is believed to be a source of heat generation, it is not excluded that the dye molecules could form aggregates that would split the LC orientation into small domains as well.

In addition to the micro-domains, critical opalescence also contributes to the scattering effect when the nematic and isotropic phases approach a critical temperature. Figure 6 shows the difference between the micro-domain (Fig. 6a) and critical opalescence (Fig. 6b) scattering mechanisms, where the physical appearance of these two mechanisms is quite distinct when observed in the near-field. A direct observation of critical opalescence in the AQ dye doped LC cell, while scanning the sample across the laser beam, shows a milky scattering structure as shown in Figure 6b.

Another contributing mechanism to the black hole effect is the enhanced absorption experienced in the isotropic phase. When the LCs are heated into the isotropic phase by the incident laser beam;

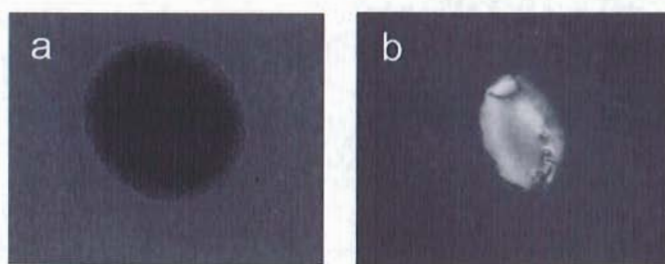


**FIGURE 6** (a) Formation of micro-domain structure immediately after switching off the He-Ne laser beam. (b) Direct observation of critical opalescence when scanning the red laser beam across the sample.

the linear absorption of the AQ/LC mixture in the isotropic phase increases. When the concentration of dye is above 0.3 wt.%, the absorption in the isotropic phase becomes significantly greater than that of the nematic phase. Figures 7(a,b) show the linear absorption spectra for two different concentrations of AQ dye in the 30  $\mu\text{m}$  thick cells (0.3 and 1.2 wt.%); the absorption in the two phases is nearly equal at 0.3 wt.% dye and almost a factor of two different for the cell with 1.2 wt.% dye. In Figure 7c, the absorption coefficients as a function of dye concentration for a laser beam polarized parallel and perpendicular to the orientation of the LCs, and the absorption coefficients measured in the isotropic phase  $\alpha_{iso}$  and  $\langle\alpha\rangle$  are shown for the wavelength 633 nm. The absorption coefficients are defined for the intensity of the beam:  $I_{out} = I_{in}\exp(-\alpha L)$  where  $I_{in}$  and  $I_{out}$  are the intensity values at the input and output of the LC cell, respectively. It is interesting to note that the measured value of the absorption coefficient in the isotropic phase is larger than the expected average value that is calculated by individual measurements of the absorption coefficients for laser beam polarization parallel and perpendicular to the orientation direction of the LC,  $\langle\alpha\rangle = (\alpha_{\parallel} + 2\alpha_{\perp})/3$  [10]. This discrepancy increases with greater dye concentrations. This is a clear indication that a large dye concentration triggers complex processes in the material, such as formation of dye aggregates with a temperature dependent “aggregation number,” as well as diffusion. It would be speculative to make more specific statements without detailed further research of this phenomenon.

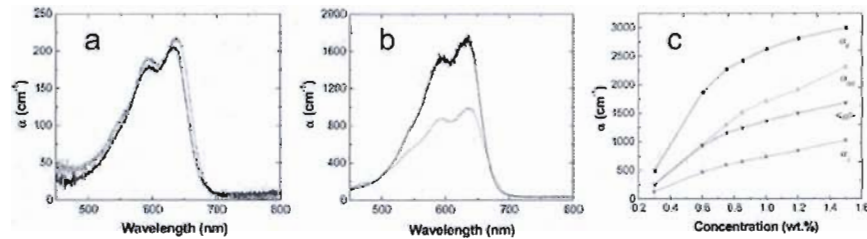


**FIGURE 7** Unpolarized absorption spectra of the dye doped LC cells as a function of concentration, (a) 0.3 wt.%, (b) 1.2 wt.%. The solid curves are the spectra measured in the isotropic phase and the dotted curves are the spectra measured in the nematic phase. (c) Absorption coefficient ( $\alpha$ ) as a function of dye concentration for a laser beam polarized parallel ( $\alpha_{\parallel}$ ) and perpendicular ( $\alpha_{\perp}$ ) to the orientation of LC.  $\alpha_{iso}$  and  $\langle\alpha\rangle$  are the measured and the evaluated absorption coefficients in the isotropic phase, respectively.

## Part 2-Switchable Reversed Diffraction

The effect of relatively high intensities on a LC cell with a large concentration of dye, 2.0 wt. % AQ, is examined in this part of the work. A CW 532 nm laser is used rather than the He-Ne because the absorption is weaker at this wavelength allowing for a more detailed analysis of the transmitted and reflected beams with less of a loss due to the strong absorbance. The same effect is observed in the red, but with a lower switching threshold intensity because of the larger linear absorption in that spectral region (see Fig. 7).

At relatively high intensities (up to  $25 \text{ kW/cm}^2$ ), when the cell is placed at the beam waist, the transmitted light through the LC cell forms concentric ring patterns, where the inner rings are fine and the outer rings are coarse, shown in Figure 8a at position  $S_2$ . This ring pattern is characteristic of self-focusing due to thermal indexing, which is the change in the index of refraction due to the inhomogeneous heating of the material, as is also the case in Figure 3c. The

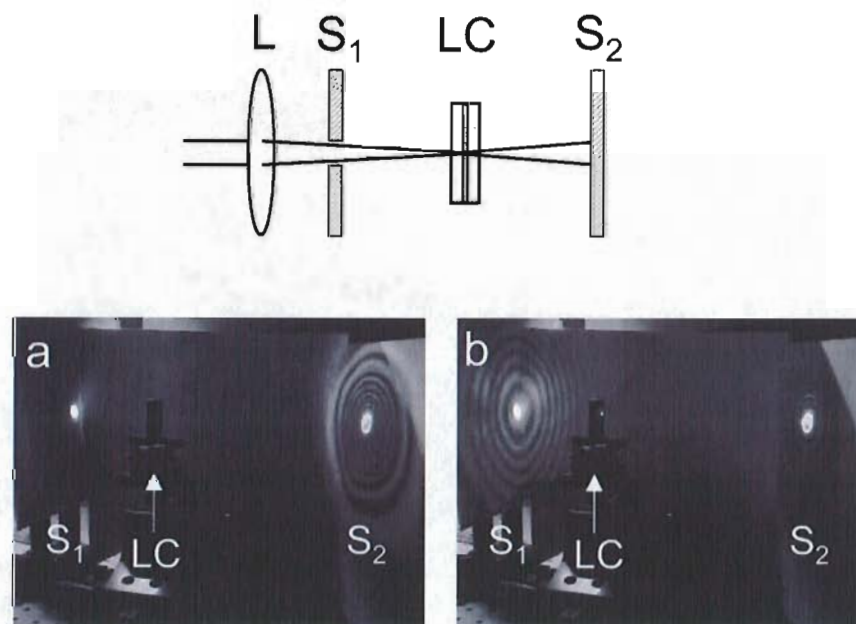


**FIGURE 8** Far-field images are the transmitted and reverse diffracted light from the dye doped LC cell. The experimental arrangement consists of a lens (L), a liquid crystal cell (LC), and screens ( $S_1$  and  $S_2$ ). The incident laser beam entered through the screen  $S_1$ .

inhomogeneous heating is due to the Gaussian profile of the laser beam. The Fresnel reflection from the cell counter-propagates along the incident beam and can be seen around the entrance hole of the screen at position  $S_1$ . The transmission increases linearly with incident power, although the transmitted intensity decreases because the ring pattern increases in diameter with increasing power.

As the incident power is increased to a threshold power  $\sim 18$  mW ( $\sim 25$  kW/cm<sup>2</sup>), an apparently instantaneous switching effect occurs, where a significant amount of the transmitted light suddenly reverses direction becoming counter-propagating (SRD). This effect is shown in Figure 8b, where the transmitted beam at position  $S_2$  is relatively weak and the backward diffracted beam at position  $S_1$  is significantly greater in intensity. Unlike the transmitted ring pattern at lower intensities, the reversed diffracted rings are of equal space and thickness. It was observed that the switching occurs due to the formation of a gaseous micro-bubble which acts as a micro-mirror as seen in Figure 9c. Even though the LCs are degassed in a vacuum chamber before making the LC cells, it may be possible that some air stays in them forming the micro-bubbles when enough heat is generated. For comparison the LCs in the nematic and isotropic states and the corresponding transmission patterns are shown in Figures 9a and 9b, respectively. Because of the spherical nature of the gas bubble, the reversed diffraction direction is independent of the angle of the incident beam. Even with the cell set at a  $70^\circ$  tilt with respect to the incident beam, the reversed diffracted beam counter-propagates along the incident beam, rather than in the direction of the Fresnel reflection. This is only true as long as the micro-bubble generated is smaller than the thickness of the cell. Micro-bubbles generated with a power level significantly greater than threshold do not allow for pure counter-propagating beams. The micro-bubbles increase in size with power, when their diameter is on the order of the thickness of the LC cell they are distorted by the cell boundaries.

In order to quantify the amount of transmitted and reversed diffracted light, transmission and reflection measurements were conducted using an integrating sphere. The light was focused onto the cell while it was mounted at the entrance port of the integrating sphere. The transmitted light was collected in the integrating sphere and the results are shown in Figure 10a. For input powers up to 10 mW ( $\sim 14$  kW/cm<sup>2</sup>) the transmission is linear. The transmission becomes nonlinear over a power range of  $\sim 10$ – $18$  mW ( $\sim 14$ – $25$  kW/cm<sup>2</sup>), indicating that the absorption is increasing. In this power range the LCs are in the isotropic state; the increased absorption corresponds with the results seen in Figure 7. At  $\sim 25$  kW/cm<sup>2</sup> there is a sudden

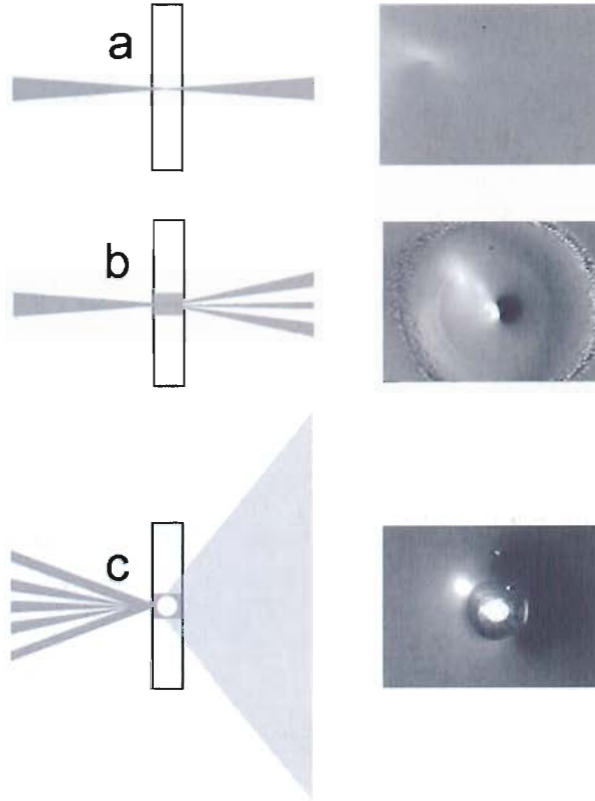


**FIGURE 9** Diagrams of the scattering effects observed as a function of input intensity and the corresponding images of the liquid crystal in the (a) nematic state, (b) isotropic state, and (c) gaseous state (presence of a micro-bubble).

increase in transmitted power, although the overall intensity is reduced as seen in Figure 8b. The transmitted light increases after the formation of the micro-bubble, because a small region of highly absorbing dye is replaced with a non-absorbing gas.

For reflection measurements, the light was focused through the integrating sphere onto the cell while it was mounted at the exit port of the integrating sphere. The Fresnel reflection was reflected back through the entrance port in order to minimize the detection of scattered light inside the integrating sphere. A bare window was used as a reference, which shows only a small amount of scatter over the power range used. Replacing the bare window with the LC cell, a sudden increase in reflected power is seen at the same power threshold as the increased transmission occurs.

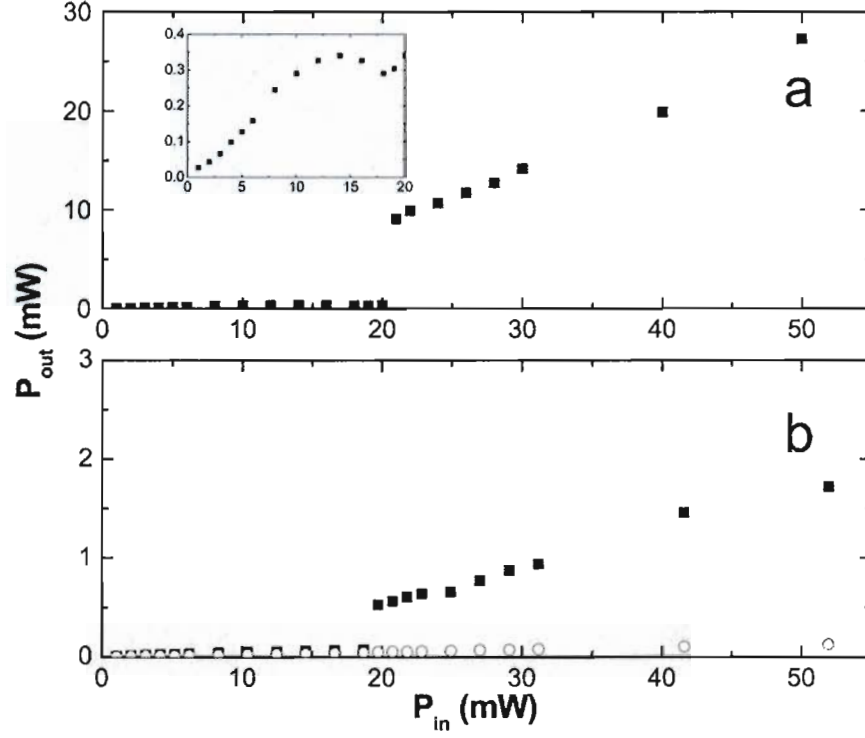


**FIGURE 10** Integrated transmitted (a) and reflected (b) powers as a function of input power (squares). The inset in trace (a) is an enlargement of the weaker input powers (0–20 mW). The open circles in trace (b) are the reflected light values from a bare window.

To verify that the intensity actually decreases although the transmitted power has been shown to increase, the hysteresis of the scattering angle (divergence) of the transmitted light is determined as a function of input power as shown in Figure 11. When increasing the power up to the threshold of reversed diffraction (18–20 mW), the angle of divergence gradually increases from 0.25 rad to 0.79 rad. When the micro-bubble forms at the threshold power, in this case  $\sim 18.5$  mW, the transmitted beam divergence suddenly jumps from 0.79 to 2.25 rad. Once switched, the beam divergence remains at 2.25 rad down to power levels (5.8 mW,  $8 \text{ kW/cm}^2$ ) that are unable to sustain the micro-bubbles. Once a micro-bubble is formed, it remains in the laser beam, even at a fraction of the threshold power required for its formation. When the laser intensity (i.e., generated surface



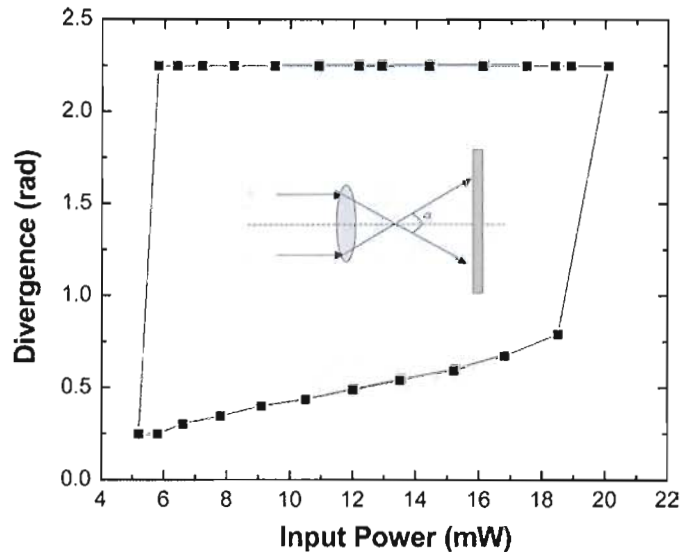


**FIGURE 11** Hysteresis of the scattering angle of the transmitted light as a function of input power. The inset is a schematic of the experimental arrangement.

tension) is too weak to hold the micro-bubble ( $< 5.8 \text{ mW}$ ) in the path of the focused beam, the bubble floats away and the transmitted beam returns to  $0.25 \text{ rad}$  divergence. The reason for the trapping of the bubble in the laser beam is related to the Marangoni Effect [11]. The gradient of heat generated in the laser beam yields a surface tension gradient. The liquid flows from regions with low surface tension to regions with a higher surface tension. For volume conservation, the bubble moves the opposite way (to fill the fluid void). When the heat generated by absorption is inadequate to generate the required surface tension, the bubble breaks loose and floats away.

## CONCLUSIONS

Two different effects have been observed in LCs with large concentrations of AQ dye depending on the incident intensity. At low intensities, the effect in which the light disappears at the output of the LC cell has been referred to as the black hole effect. This effect is due to micro-domain scatter, critical opalescence, and enhanced absorption in the isotropic phase. At high intensities, SRD occurs when photo-induced micro-bubbles reflect (or diffract) light in a counter-propagating

direction, regardless of the angle of incidence of the laser beam. A highly concentrated dye doped LC cell allows for the ability to manipulate light over a large range of intensities using different physical mechanisms in a single cell.

## REFERENCES

- [1] Tabiryan, N. V., Zel'dovich, B. Ya., & Sukhov, A. V. (1986). *Special Issue of Mol. Cryst. Liq. Cryst.*, 136(1), 1.
- [2] Khoo, I. C. (1994). *Liquid Crystals: Physical Properties and Nonlinear Optical Phenomena*, Wiley Interscience: New York.
- [3] Simoni, F. (1997). *Nonlinear Optical Properties of Liquid Crystals and Polymer Liquid Crystals*, World Scientific: Singapore.
- [4] Janossy, I., Lloyd, A. D., & Wherrett, B. S. (1990). *Mol. Cryst. Liquid Cryst.*, 179, 1.
- [5] Khoo, I. C., Chen, P. H., Shih, M. Y., Shishido, A., & Slussarenko, S. (2001). *Mol. Cryst. Liq. Cryst.*, 358, 1.
- [6] Marrucci, L. (2002). *Liquid Crystals Today*, 11(3), 6.
- [7] Tabiryan, N. V., Hrozhyk, U. A., Margaryan, H. L., Mora, M. J., Nersisyan, S. R., & Serak, S. V. (2002). *Mat. Res. Soc. Symp. Proc.*, 709, 91.
- [8] Tabiryan, N. V., Serak, S. V., & Grozhik, V. A. (2003). *J. Opt. Soc. Am. B*, 20(3), 1.
- [9] Tabiryan, N. V. & Nersisyan, S. (2002). *Opt. Eng.*, 41, 2876.
- [10] Sutherland, R. L. (2002). *JOSA B*, 19, 2995.
- [11] Velarde, M. G. & Zeytourian, R. K. (Eds.) (2002). *Interfacial Phenomena and the Marangoni Effect*, Springer: New York.



Copyright of *Molecular Crystals & Liquid Crystals* is the property of Taylor & Francis Ltd and its content may not be copied or emailed to multiple sites or posted to a listserv without the copyright holder's express written permission. However, users may print, download, or email articles for individual use.